RSC Advances

PAPER

View Article Online
View Journal | View Issue



Cite this: *RSC Adv.*, 2018, **8**, 40687

# $^{19}$F multiple-quantum coherence NMR spectroscopy for probing protein–ligand interactions†

Anna Zawadzka-Kazimierczuk,*[ab] Mate Somlyay,[a] Hanspeter Kaehlig,[c] George Iakobson,[d] Petr Beier[d] and Robert Konrat*[a]

Received 10th November 2018
Accepted 28th November 2018

DOI: 10.1039/c8ra09296f

rsc.li/rsc-advances

A new $^{19}$F NMR method is presented which can be used to detect weak protein binding of small molecules with up to mM affinity. The method capitalizes on the synthetic availability of unique $SF_5$ containing compounds and the generation of five-quantum coherences (5QC). Given the high sensitivity of 5QC relaxation to exchange events (*i.e.* reversible protein binding) fragments which bind to the target with weak affinity can be identified. The utility of the method in early stage drug discovery programs is demonstrated with applications to two model proteins, the neurotoxic NGAL and the prominent tumor target β-catenin.

## Introduction

Fragment-based drug discovery (FBDD) has become a cornerstone of modern drug discovery programs. Several compounds have entered clinical trials[1,2] and, as for now, two of them are already used for patient treatment.[3,4] Particularly noteworthy is that FBDD strategies provide valid starting points for drug discovery even in cases where conventional high throughput screens (HTS) fail.[5] During the course of a fragment-based drug discovery program weak binders in the 100–300 Da range are initially identified which are subsequently evolved in an iterative manner into larger compounds with higher binding affinities and better target selectivity. For the identification of initial hits several biophysical techniques exist, among them NMR spectroscopy is unique as it provides reliable quantitative binding information over a wide range of dissociation constants ($K_D$). Subsequent fragment optimization either by fragment merging (linking different fragments) or fragment extension (introducing additional functional groups) exploits chemical information provided by structural studies using (mostly) X-ray crystallography and/or NMR spectroscopy.[6] Additionally, lead compounds identified in early stages of the drug design process are sometimes used as reporter ligands for either screening additional chemical libraries or validate optimized follow-up hits.[7]

Ligand-based NMR spectroscopy is particularly powerful in drug discovery to identify small molecule binders. First, contrary to methods based on observation of protein molecules, only very little protein material is required and even allows for the examination of ligand mixtures. Second, protein–ligand interaction is a dynamic process where the protein exchanges between the apo (ligand free) and the ligand-bound state. In case of weak interaction both states exist leading to averaging of NMR observables and weighted by their respective populations which in turn depend on the dissociation constant ($K_D$) of the complex and the concentrations. In principle, monitoring and quantification of protein–ligand binding by NMR spectroscopy can be achieved by chemical shift measurements or nuclear Overhauser enhancement spectroscopy (NOESY). A large and diverse set of different NMR techniques exist which exploit these possibilities,[8] among others saturation transfer difference (STD)[9] or WaterLOGSY.[10] Finally, in early stages of the drug design process ligand binding affinities are weak (μM $K_D$'s) leading to fast exchange between the free and bound state which can be efficiently probed by Carr–Purcell–Meiboom–Gill (CPMG) relaxation dispersion methodology.[11] Furthermore, it has been shown that ligand-observed CPMG measurements can be effectively used not only for ligand screening but also to determine, for example, lifetimes of drug–target complexes.[12]

Among the various ligand-based methods, $^{19}$F NMR spectroscopy has gained significant attention due to various advantages: the NMR-active $^{19}$F isotope has high gyromagnetic ratio and 100% natural isotope abundance, assuring high

[a]*Department of Structural and Computational Biology, Max F. Perutz Laboratories, University of Vienna, Vienna Biocenter Campus 5, A-1030 Vienna, Austria*

[b]*Biological and Chemical Research Centre, Faculty of Chemistry, University of Warsaw, Żwirki i Wigury 101, 02-089 Warsaw, Poland*

[c]*Institute of Organic Chemistry, University of Vienna, Währinger Strasse 38, A-1090 Vienna, Austria*

[d]*Institute of Organic Chemistry and Biochemistry of the Czech Academy of Sciences, Flemingovo nam. 2, 160 00 Prague, Czech Republic. E-mail: anzaw@chem.uw.edu.pl; Robert.Konrat@univie.ac.at*

† Electronic supplementary information (ESI) available: Additional information on 5Q coherence generation, doublet components merging procedure, relaxation simulation, chemical synthesis of ligand **1**. See DOI: 10.1039/c8ra09296f

sensitivity. Fluorine has a very large chemical shift dispersion that allows the investigation of large compound mixtures in a high throughput manner.[7,13–17] NMR detection is straightforward as the spectra are devoid of background signals from solvents and proteins. Last and most importantly, the chemical shifts and the relaxation properties of the fluorine nuclei are extremely sensitive to small changes of the chemical environment (binding to target).[18] Furthermore, fluorine incorporation into drugs is an established optimization strategy in medicinal chemistry.[19,20] Insertion of a fluorine atom in a molecule can change the p$K_a$, log $P$, conformation and metabolism of a compound. Owing to these factors, 20% of all drugs contain at least one fluorine atom.

Particularly interesting in that respect is the pentafluorosulfanyl ($SF_5$) group, which was introduced in small molecules first in 1960.[21] It is a peculiar chemical group with octahedral geometry. The group consists of one axial and four equatorial fluorines, which give rise to a quintet and a doublet ($J \approx 150$ Hz) in the $^{19}$F NMR spectra, respectively. The $SF_5$ group is very often compared to the $CF_3$ group: it is sterically demanding and highly electronegative ($\sigma_p = +0.68$ *versus* +0.54 for $CF_3$). It has high dipole moment ($\mu = 3.4$ D *versus* 2.6 for $CF_3$) and high lipophilicity (log $P$ = 2.55),[22–25] which are usually opposing properties. The review of Welch and Savoie is an excellent summary of the various applications of $SF_5$ compounds.[26]

In the present study we exploit this highly symmetric spin system for the generation of high order spin states (multiple quantum coherences) and explore the applicability to increase the sensitivity of $^{19}$F-based NMR screening methods. Specifically, we demonstrate that this novel $^{19}$F NMR methodology is able to detect weak affinity binders typically found in early stages of drug developmental programs. This could be applied in fragment screening where weak binders are used as spy ligands[7] to probe additional chemical libraries and follow the chemical optimisation process.

## Results and discussion

Our new method relies on the change of relaxation of the ligand upon binding to a protein. In case of a ligand reversibly binding to a protein target the observed relaxation ($R'$) is the average of relaxation of the ligand in a free form ($R_L$) and bound form ($R_{LP}$):

$$R' = p_L R_L + p_{LP} R_{LP} \quad (1)$$

where $p_L$ and $p_{LP}$ are populations of the free and bound form, respectively. Ligand relaxation in the bound state is largely governed by the increased correlation (tumbling) time of the complex compared to the free ligand. Additional intermolecular interactions might contribute to the relaxation of the bound state.

However, there is another effect that contributes to the relaxation and stems from exchange contribution to the linewidth. In case of a fast two-site exchange process between free and bound state the exchange contribution is given by $R_{ex} = p_L p_{LP} \Delta\omega^2 / k_{ex}$ where $k_{ex}$ is the exchange rate, $\Delta\omega$ is resonance frequency difference between free and bound states. Depending on the chemical shift changes upon binding this can even become the dominating contribution to transverse $^{19}$F relaxation.[27]

Exchange processes, however, can only be detected by CPMG provided that populations and rates are within a narrow window for observation of relaxation dispersion experiments. Instead, measuring the decay of multiple quantum coherences has been proposed as an attractive alternative[28] as these higher order coherences evolve as the sum of individual chemical shifts. For example, in case of symmetric spin systems the multiple-quantum coherence chemical shift difference, $\Delta\omega_{MQ}$ depends on the coherence order $n$ and the chemical shift difference observed for single quantum coherence, $\Delta\omega_{MQ} = n\Delta\omega$. In this case, the exchange contribution to the linewidth is given by $R_{ex,MQ} = p_L p_{LP} n^2 \Delta\omega^2 / k_{ex}$. Thus, while the observed ligand relaxation rate in the presence of target can be small in case of single quantum coherences, the relaxation of multiple-quantum coherence could be sizeable. This effect has been already exploited in fluorine double-quantum relaxation measurements.[29]

Here we exploit the dependence of exchange contributions to the linewidth by $n^2\Delta\omega^2$ through the generation of five quantum coherences (5QC) in $SF_5$-containing ligands and probe their binding to protein targets. The new experiment allows probing of protein ligand binding events involving smaller populations of the bound state than would be possible by existing single-quantum coherence techniques. The $^{19}$F 5Q pulse scheme for probing of $^{19}$F ligand binding to protein targets is illustrated in Fig. 1. In $SF_5$ group axial and equatorial fluorines are

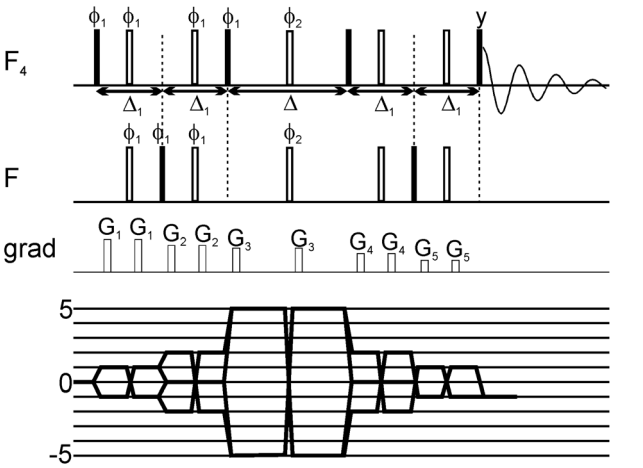


Fig. 1 Scheme of the 5Q pulse sequence for $T_2$ measurements of the $SF_5$ system, together with coherence transfer pathway. All pulses were selective shaped pulses. The pulses acting on one type of fluorine nuclei (F or $F_4$ group) were sinc-shaped; their length was set to 250 μs and offset was set on the frequency of the group. The pulses applied simultaneously on F and $F_4$ groups were cosine-modulated sinc-shaped pulses; their length was 250 μs and offset was set in the middle between the two frequencies. the $\Delta_1$ delay was set to 6.28 ms and the relaxation delay $\Delta$ was incremented. The pulse phases were set to $x$, unless shown explicitly. On the phase $\phi_1$ a 10-step phase cycle was performed to select the coherence of ±5 order during the multiple-quantum period. Additionally, on the phase $\phi_2$ a 4-step phase cycle was performed.

 

magnetically non-equivalent and can thus be excited independently from each other using appropriate shaped pulses. Key to the pulse scheme is the efficient generation of five quantum coherence given by $16F^{a}_{+}F^{1}_{+}F^{2}_{+}F^{3}_{+}F^{4}_{+}$, where $F^{a}$ indicates the axial $^{19}$F and 1, 2, 3 and 4 are labels for the equivalent equatorial fluorine spins. Here we adapted a strategy originally proposed by Kay and co-workers.[28] Instead of directly generating $16F^{a}_{x}F^{1}_{x}F^{2}_{x}F^{3}_{x}F^{4}_{x}$, which would be an unfavourable superposition of different $^{19}$F higher order terms we preserve most of the signal by selecting the following term $16F^{a}_{x}F^{1}_{x}F^{2}_{y}F^{3}_{y}F^{4}_{y}$ (as well as other symmetry-related linear combinations). In brief, this is achieved by generating a single anti-phase term $2F^{a}_{z}F^{1}_{x}$ during the first $\Delta_1$ period (see Fig. 1), followed by conversion into $2F^{a}_{y}F^{1}_{x}$ and evolution into $16F^{a}_{x}F^{1}_{x}F^{2}_{z}F^{3}_{z}F^{4}_{z}$ and after a $\pi/2$ pulse conversion into $16F^{a}_{x}F^{1}_{x}F^{2}_{y}F^{3}_{y}F^{4}_{y}$ (and corresponding terms for 2,3,4) which finally relaxes during the relaxation period $\Delta$. After the relaxation period the signal is transferred back to the sensitive (magnetically equivalent) $F_4$ group for detection. The efficiency of the magnetization transfer and generation of 5Q coherences was carefully checked using 2D NMR spectroscopy (see ESI†). Quality and efficacy of 5Q coherence generation was assessed based on peak position and lineshape of the cross peak and demonstrated that phase cycling for removal of undesirable coherence pathways was successful.

After establishing that $^{19}$F 5Q coherences can be efficiently created and as a first application of the new methodology we have studied the binding of small $SF_5$-substituted small molecule compounds to proteins and investigated (quantitatively) relaxation changes of 1Q and 5Q coherences upon binding to protein targets. Two $SF_5$-ligands were selected. 5-(pentafluoro-$\lambda^6$-sulfanyl)-1,3-benzoxazole-2(3*H*)-thione is denoted below as ligand **1**, and **2**-bromo-4-(pentafluoro-$\lambda^6$-sulfanyl)aniline is denoted as ligand **2** (see Fig. 2). Their binding to neutrophil gelatinase-associated lipocalin (NGAL) and β-catenin was studied by $^{19}$F NMR. In the $^{19}$F NMR spectrum of the $SF_5$ group the four equatorial fluorines give rise to an intense doublet while the axial fluorine atom appears as a complex quintet. Due to sensitivity consideration we prefer to record the equatorial $F_4$ doublet. Arguably it would be beneficial to observe the $^{19}$F signal under homonuclear decoupling conditions. In reality, however, homonuclear decoupling schemes can be challenging for the general user to set up and often do not provide significant sensitivity gains largely due to relaxation losses during acquisition and decoupler sideband interferences. Since we were aiming at a robust and easy to implement experimental set-up avoiding sophisticated parameter optimization we opted for a computational strategy to eliminate homonuclear scalar couplings. Specifically, we pursue a shifting-merging strategy. Details are explained in the ESI.†

Decaying 1Q and 5Q spectra of the $F_4$ group of ligand **1** at the absence and presence of protein are shown in Fig. 3. The dependence of peak intensity on relaxation delay, together with the exponentially decaying trends obtained for 1Q and 5Q relaxation under different conditions (protein-free *vs.* protein-bound) are shown in Fig. 4. The analysis of the curves reveals that the 5Q relaxation is more sensitive to protein binding than the relaxation of the 1Q term. As expected relaxation is more pronounced in the protein-bound state as a consequence of the larger correlation time of the bound state (protein complex) and due to exchange contributions to the $^{19}$F linewidth resulting from the reversible binding process. As we described above exchange contributions of multiple-quantum coherences scale with the square of the coherence order. In case of 5Q coherences sizeable differential contributions can thus be expected.

Differential relaxation of 5Q and 1Q was analysed as a function of protein concentration and is illustrated in Fig. 5, which shows the relative change of the relaxation rates normalized to the values of the apo-state ($\Delta R/R_{lig}$) and its dependence on the protein concentration. It is evident from the figure that increasing protein concentration leads to a sizeable difference of 5Q and 1Q relaxation; $\Delta R/R_{lig}$ is typically about two times larger for 5Q than for 1Q. At low protein concentration relative relaxation changes are comparable for 5Q and 1Q coherences.

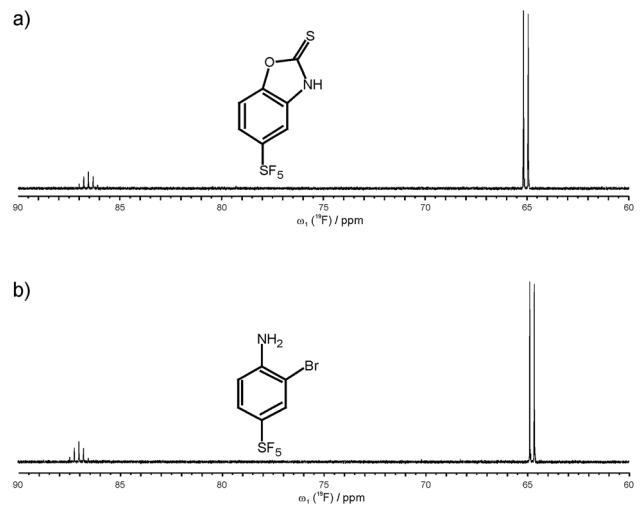


Fig. 2 Chemical structure and $^{19}$F NMR spectrum of ligand **1**, 5-(pentafluoro-$\lambda^6$-sulfanyl)-1,3-benzoxazole-2(3*H*)-thione (a), and ligand **2**, 2-bromo-4-(pentafluoro-$\lambda^6$-sulfanyl)aniline (b).

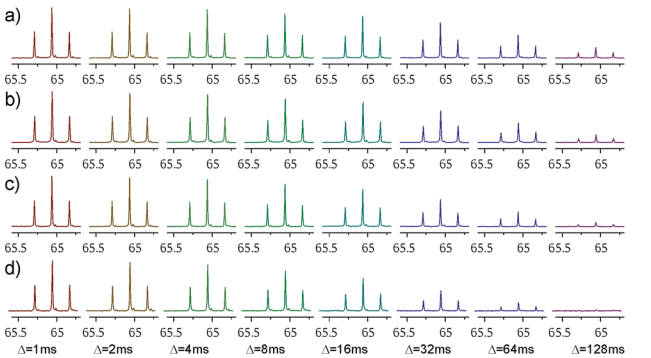


Fig. 3 Decaying spectra of the $F_4$ group signal (after the merging procedure), with increasing relaxation delay $\Delta$. panels (a) and (c) show the ligand **1** alone (at 1 mM concentration), while panels (b) and (d) ligand **1** with 8 μM of NGAL protein. Panels (a) and (b) show decays of 1Q coherence, while panels (c) and (d) show decays of 5Q coherence.

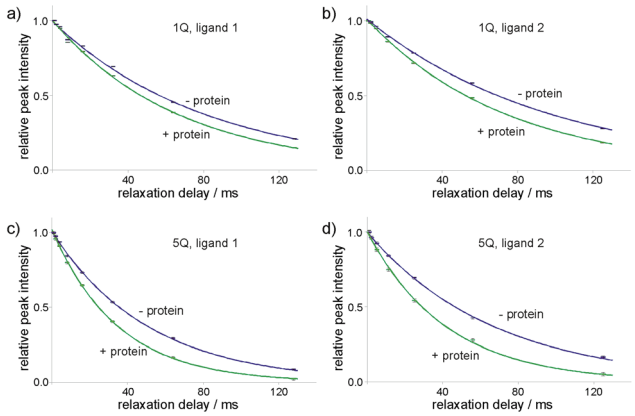


Fig. 4 Decay of the merged $F_4$ group peak intensity with increasing relaxation delay Δ, together with the exponential decay trends. Data are shown for ligand **1** (panels (a) and (c)) and ligand **2** (panels (b) and (d)). Relative peak intensities of 1Q (panels (a) and (b)) and 5Q (panels (c) and (d)) coherence peaks are shown. Purple markers and lines correspond to the data for the ligands alone, green ones correspond to the ligands with added protein. The protein concentration for ligand **1** was 8 μM and for ligand **2**: 3 μM.

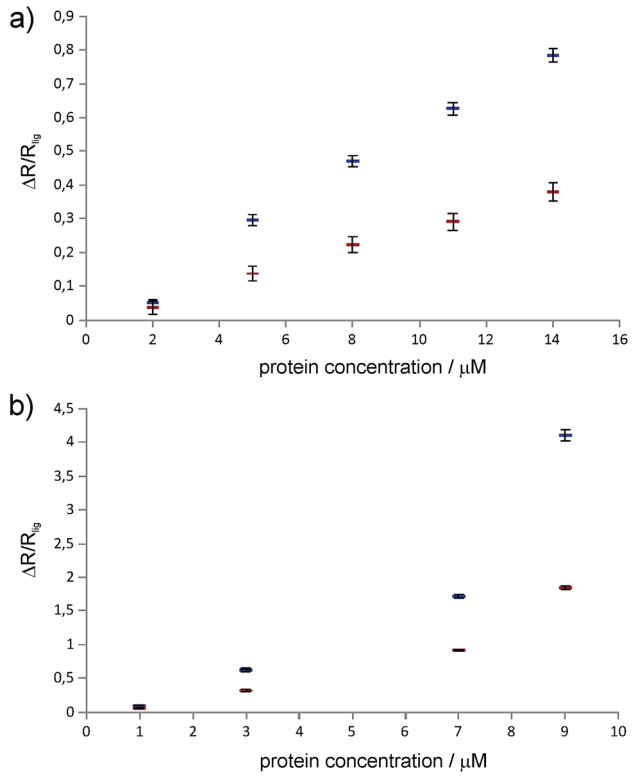


Fig. 5 Relative change of 1Q (red markers) and 5Q (blue markers) relaxation rates of the ligand (with respect to the relaxation rate of the ligand alone) at different protein concentrations. (a) Ligand **1** with NGAL protein, (b) ligand **2** with β-catenin protein.

In contrast, at higher protein concentration significant differences are found. Clearly, 5Q coherences are more sensitive to protein binding than 1Q coherences. In other words, 5Q coherences exhibit the same relative changes in the $T_2$ value as the 1Q coherence but already at significantly smaller protein concentrations. Additionally, closer inspection of Fig. 5a shows that NGAL/ligand **1** displays a linear dependence of $\Delta R/R_{lig}$ *vs.* protein concentration indicating that the measured relaxation rate is a population average of contributions from the apo and bound state, respectively. Conversely, the $\Delta R/R_{lig}$ analysis for β-catenin/ligand **2** clearly reveals non-linearity (Fig. 5b). This could be due to exchange contributions (between free and bound state) and which is typically found for weakly binding ligands. In this case the exchange contribution is given by $p_L$-$p_{LP}k_{ex}\Delta\omega^2/k_{ex}$, and $p_Lp_{LP}$ does not scale linearly with increasing protein concentration. However, given the low affinity ($K_D$ is high μM) of the β-catenin/ligand **2** complex the population of the bound state is rather small and at low protein concentrations the ligand exists predominantly in the free state ($p_L \approx 1.0$) and thus the product of the populations $p_Lp_{LP} \approx p_{LP}$. The expected non-linearity (due to $p_Lp_{LP}$) occurs only at substantially higher protein concentrations (simulations are given in the ESI†).

Therefore we concluded that the observed non-linear concentration dependence of β-catenin is due to protein oligomerization (aggregation) leading to a substantial increase in the relaxation rate of the bound state. This is also in agreement with the empirical observation that β-catenin displays low solubility and tends to aggregate in solution. The superior sensitivity of the proposed methodology to probe protein binding even at low protein concentrations might thus become important for future NMR-supported programs aiming at β-catenin inhibitors as anti cancer drugs.

The 5Q experiment is of course less sensitive (in terms of signal-to-noise ratio) than the 1Q experiment. The estimated 5Q/1Q sensitivity ratio is about 10%. Therefore the number of scans needed for data acquisition should be increased to obtain sufficient sensitivity. In our case the number of scans employed for 5Q experiment for ligand **1** (whose concentration was 1 mM) was 40 which corresponds to *ca.* 14 minutes of the total measurement time to record the data for 8 different relaxation delays (from 1 ms up to 128 ms). For ligand **2** (0.5 mM concentration) the number of scans was increased to 160, which corresponds to *ca.* 49 minutes of the total measurement time (for 7 different relaxation delays, from 1 ms to 125 ms). The issue of sensitivity is being constantly alleviated with the development of NMR equipment. Despite lower signal-to-noise ratio, 5Q experiment is very powerful in terms of possibility of detection of binding event. In this case the difference between relaxation rates of a free ligand and ligand in a presence of protein is much larger than in the case of 1Q experiment.

Of course, the proposed 5Q experiment requires presence of the $SF_5$ group in the ligand. Therefore we expect that the main application would be competition experiments. The $SF_5$-containing molecule can be used as a spy to report binding events of other ligands present in the solution. High specificity of the method allows screening large sets of ligands at a time, including also those containing fluorine atom(s). The observed spectrum would always contain only one signal, which makes the analysis straightforward.

# Experimental

### NMR samples

The NMR samples used in our measurements were 450 μL in volume and contained 5% DMSO-D6 to ensure lock signal and proper solubility of the ligands. The samples were prepared using 2–14 μM NGAL with 1 mM ligand **1** and 1–9 μM beta-catenin with 500 μM ligand **2**.

### NMR experiments

All NMR experiments were performed on a Bruker Avance III HD+600 MHz spectrometer equipped with an X(CPF) $^{1}$H-decoupled gradient (QP) probe and Bruker Avance III HDX 700 MHz spectrometer equipped with Cryo-QCI-F probe, operating at $^{19}$F frequencies of 564 MHz and 659 MHz, respectively. The acquisition parameters were gathered in the Table 1.

### Protein expression and purification

Recombinant human beta-catenin (bCat) was produced as a $H_6$-MBP-3C-bCat$^{141-781}$ construct from a petM44 plasmid in *E. coli* BL21(DE3) in LB media. After reaching an $OD_{600} = 0.7–0.9$, the cultures were put for 5 min on ice before induction with 0.4 mM IPTG (isopropyl-β-D-1-thiogalactopyranoside) at 18 °C. After 20 hours of expression, the cells were collected by centrifugation and resuspended in 40 mL buffer containing 20 mM Tris, 150 mM NaCl, 5 mM β-mercaptoethanol, 1 mM benzamidine and protease inhibitor (Roche cOmplete Mini, EDTA free). After sonication and centrifugation, proteins were purified by $Ni^{2+}$ affinity chromatography (HisTrap Chelating HP, 5 mL, GE Healthcare). The obtained protein (~60 μM) was diluted to a concentration of 5 μM and cleaved overnight at 4 °C with 3C protease (20 mM Tris, 150 mM NaCl, 1% glycerol, 2 mM β-mercaptoethanol). The solution was again loaded onto a $Ni^{2+}$ column. The cleaved tag, the His6-tagged 3C protease and the bCat$^{141-781}$ was eluted with a gradient (0–200 mM imidazole) of 20 CV. Appropriate fractions were loaded onto a gel filtration column equilibrated in 20 mM Tris, 150 mM NaCl, 0.5 mM DTT, pH = 7.45 (HiLoad 26/60 Superdex 200pg, GE Healthcare). Beta-catenin containing fractions were diluted to 5 μM concentration and stored at −20 °C.

Recombinant neutrophil gelatinase-associated lipocalin (NGAL) was produced as a $H_6$-TEV-NGAL construct from a petM11 plasmid in BL21pLysS cells in LB media. After reaching an $OD_{600} = 0.8$, protein expression was induced with 0.8 mM IPTG (isopropyl-β-D-1-thiogalactopyranoside) at 30 °C. After overnight expression, the cells were collected by centrifugation and resuspended in 40 mL PBS buffer. After sonication and centrifugation, proteins were purified by $Ni^{2+}$ affinity chromatography (HisTrap Chelating HP, 5 mL, GE Healthcare). The obtained protein was dialyzed overnight to Tris buffer (20 mM Tris, 50 mM NaCl, pH = 7.4). The protein was cleaved with TEV-protease overnight in Tris buffer (1 mM DTT, 0.5 mM EDTA), and loaded on a gel filtration column (HiLoad 16/60 Superdex 75pg, GE Healthcare). NGAL-containing fractions were pooled and concentrated to 0.5 mL, and the protein was denatured with 0.5 g guanidine hydrochloride. After 20 minutes incubation at 70 °C, the protein was loaded on a desalting column (PD10, Sephadex™ G-25 M, GE Healthcare) equilibrated with 6 M guanidine hydrochloride. The denatured protein was dialyzed to Tris buffer. After two days, the precipitates were centrifuged and the protein was stored at −20 °C.

# Conclusions

In summary, we have presented a $^{19}$F 5Q relaxation experiment for probing of ligand binding to protein targets. The experiment offers superior sensitivity compared to conventional $^{19}$F 1Q methodologies and thus allows the identification and characterization of weak binders typically found in early stages of drug discovery programs. Exchange line broadening due to reversible protein binding can be a significant contribution to transverse relaxation and is thus exploited in NMR ligand screening. The potentially beneficial effect of exchange contributions to NMR probing of ligand screening has been extensively discussed and reviewed by Dalvit and co-workers.[18] As the chemical exchange contribution to the transverse relaxation scales with the square of the coherence order, this term in the proposed 5Q experiment can be as much as twenty-five times larger than the corresponding term in the typically performed 1Q experiment. The significant increase in sensitivity will be advantageous in drug screening programs as ligand binding events can be detected at lower populations of the protein bound state. This substantially decreases the required amount of protein material, which is still a limiting factor in large scale screening initiatives. Consequently, we are proposing to use this $^{19}$F 5Q methodology for searching $SF_5$ reporter molecules as potential spy compounds for the screening of chemical libraries. Furthermore, versatile synthetic approaches exist to $SF_5$-containing chemical scaffolds offering access to diversity-oriented fragment screening libraries. As such, this novel $^{19}$F 5Q approach provides a rich avenue in drug discovery programs where protein availability and low concentration of protein ligand complexes are limiting.

Table 1 Acquisition parameters for 1D experiments

| Ligand | Coherence order | Number of scans | Relaxation delays (Δ), ms | Spectral width, Hz | Number of time-domain points |
|---|---|---|---|---|---|
| Ligand **1** | 1Q | 4 | 1, 2, 4, 8, 16, 32, 64, 128 | 65 789 | 32 768 |
| | 5Q | 40 | 1, 2, 4, 8, 16, 32, 64, 128 | 65 789 | 32 768 |
| Ligand **2** | 1Q | 16 | 1, 2.2, 5, 11.2, 25, 55.9, 125 | 65 789 | 32 768 |
| | 5Q | 160 | 1, 2.2, 5, 11.2, 25, 55.9, 125 | 65 789 | 32 768 |

## Conflicts of interest

There are no conflicts to declare.

## Acknowledgements

This work was supported by the Initial Training Network, FLUOR21, funded by the FP7 Marie Curie Actions of the European Commission (FP7-PEOPLE-2013-ITN-607787) and the Austrian Science Fund Grant (W1258), DK: "Integrative Structural Biology". A. Z.-K. was supported by an FWF Lise-Meitner Postdoctoral Fellowship (M 2084). This work was financially supported by the Czech Academy of Sciences (RVO: 61388963). The authors thank prof. Andrzej Ejchart of Institute of Biochemistry and Biophysics of the Polish Academy of Sciences, for his valuable suggestions.

## References

1 J. Tsai, J. T. Lee, W. Wang, J. Zhang, H. Cho, S. Mamo, R. Bremer, S. Gillette, J. Kong, N. K. Haass, K. Sproesser, L. Li, K. S. M. Smalley, D. Fong, Y.-L. Zhu, A. Marimuthu, H. Nguyen, B. Lam, J. Liu, I. Cheung, J. Rice, Y. Suzuki, C. Luu, C. Settachatgul, R. Shellooe, J. Cantwell, S.-H. Kim, J. Schlessinger, K. Y. J. Zhang, B. L. West, B. Powell, G. Habets, C. Zhang, P. N. Ibrahim, P. Hirth, D. R. Artis, M. Herlyn and G. Bollag, *Proc. Natl. Acad. Sci. U. S. A.*, 2008, **105**, 3041–3046.

2 D. A. Erlanson, S. W. Fesik, R. E. Hubbard, W. Jahnke and H. Jhoti, *Nat. Rev. Drug Discovery*, 2016, **15**, 605–619.

3 G. Bollag, J. Tsai, J. Zhang, C. Zhang, P. Ibrahim, K. Nolop and P. Hirth, *Nat. Rev. Drug Discovery*, 2012, **11**, 873–886.

4 A. J. Souers, J. D. Leverson, E. R. Boghaert, S. L. Ackler, N. D. Catron, J. Chen, B. D. Dayton, H. Ding, S. H. Enschede, W. J. Fairbrother, D. C. S. Huang, S. G. Hymowitz, S. Jin, S. L. Khaw, P. J. Kovar, L. T. Lam, J. Lee, H. L. Maecker, K. C. Marsh, K. D. Mason, M. J. Mitten, P. M. Nimmer, A. Oleksijew, C. H. Park, C.-M. Park, D. C. Phillips, A. W. Roberts, D. Sampath, J. F. Seymour, M. L. Smith, G. M. Sullivan, S. K. Tahir, C. Tse, M. D. Wendt, Y. Xiao, J. C. Xue, H. Zhang, R. A. Humerickhouse, S. H. Rosenberg and S. W. Elmore, *Nat. Med.*, 2013, **19**, 202–208.

5 P. J. Hajduk and J. Greer, *Nat. Rev. Drug Discovery*, 2007, **6**, 211–219.

6 P. J. Hajduk, J. C. Mack, E. T. Olejniczak, C. Park, P. J. Dandliker and B. A. Beutel, *J. Am. Chem. Soc.*, 2004, **126**, 2390–2398.

7 C. Dalvit, P. E. Fagerness, D. T. A. Hadden, R. W. Sarver and B. J. Stockman, *J. Am. Chem. Soc.*, 2003, **125**, 7696–7703.

8 B. Meyer and T. Peters, *Angew. Chem., Int. Ed.*, 2003, **42**, 864–890.

9 M. Mayer and B. Meyer, *Angew. Chem., Int. Ed.*, 1999, **38**, 1784–1788.

10 C. Dalvit, P. Pevarello, M. Tato, M. Veronesi, A. Vulpetti and M. Sundström, *J. Biomol. NMR*, 2000, **18**, 65–68.

11 P. J. Hajduk, E. T. Olejniczak and S. W. Fesik, *J. Am. Chem. Soc.*, 1997, **119**, 12257–12261.

12 T. Moschen, S. Grutsch, M. A. Juen, C. H. Wunderlich, C. Kreutz and M. Tollinger, *J. Med. Chem.*, 2016, **59**, 10788–10793.

13 C. Dalvit, *Prog. Nucl. Magn. Reson. Spectrosc.*, 2007, **51**, 243–271.

14 C. Dalvit, N. Mongelli, G. Papeo, P. Giordano, M. Veronesi, D. Moskau and R. Kümmerle, *J. Am. Chem. Soc.*, 2005, **127**, 13380–13385.

15 C. Dalvit, A. D. Gossert, J. Coutant and M. Piotto, *Magn. Reson. Chem.*, 2011, **49**, 199–202.

16 C. Dalvit, E. Ardini, M. Flocco, G. P. Fogliatto, N. Mongelli and M. Veronesit, *J. Am. Chem. Soc.*, 2003, **125**, 14620–14625.

17 C. Dalvit, M. Flocco, S. Knapp, M. Mostardini, R. Perego, B. J. Stockman, M. Veronesi and M. Varasi, *J. Am. Chem. Soc.*, 2002, **124**, 7702–7709.

18 C. Dalvit and M. Piotto, *Magn. Reson. Chem.*, 2017, **55**, 106–114.

19 K. Müller, C. Faeh and F. Diederich, *Science*, 2007, **317**, 1881–1886.

20 H.-J. Böhm, D. Banner, S. Bendels, M. Kansy, B. Kuhn, K. Müller, U. Obst-Sander and M. Stahl, *ChemBioChem*, 2004, **5**, 637–643.

21 W. A. Sheppard, *J. Am. Chem. Soc.*, 1960, **82**, 4751–4752.

22 W. A. Sheppard, *J. Am. Chem. Soc.*, 1962, **84**, 3072–3076.

23 R. W. Taft, S. Ehrenson, I. C. Lewis and R. E. Click, *J. Am. Chem. Soc.*, 1959, **81**, 5352–5361.

24 L. J. Sæthre, N. Berrah, J. D. Bozek, K. J. Børve, T. X. Carroll, E. Kukk, G. L. Gard, R. Winter and T. D. Thomas, *J. Am. Chem. Soc.*, 2001, **123**, 10729–10737.

25 J. E. True, T. D. Thomas, R. W. Winter and G. L. Gard, *Inorg. Chem.*, 2003, **42**, 4437–4441.

26 P. R. Savoie and J. T. Welch, *Chem. Rev.*, 2015, **115**, 1130–1190.

27 C. Dalvit and A. Vulpetti, *Chem. - Eur. J.*, 2016, **22**, 7592–7601.

28 T. Yuwen, P. Vallurupalli and L. E. Kay, *Angew. Chem., Int. Ed.*, 2016, **55**, 11490–11494.

29 C. Dalvit and A. Vulpetti, *Magn. Reson. Chem.*, 2012, **50**, 592–597.

 